Modelling and testing the x-ray performance of CCD and CMOS APS detectors using numerical finite element simulations

Conference or Workshop Item

Modelling and testing the x-ray performance of CCD and CMOS APS detectors using numerical finite element simulations

Daniel P. Weatherill[a]*, Konstantin D. Stefanov[a], Thomas A. Greig[b] and Andrew D. Holland[a]
[a]Centre for Electronic Imaging, The Open University, UK;
[b]e2v Technologies, UK

ABSTRACT

Pixellated monolithic silicon detectors operated in a photon-counting regime are useful in spectroscopic imaging applications. Since a high energy incident photon may produce many excess free carriers upon absorption, both energy and spatial information can be recovered by resolving each interaction event. The performance of these devices in terms of both the energy and spatial resolution is in large part determined by the amount of diffusion which occurs during the collection of the charge cloud by the pixels. Past efforts to predict the X-ray performance of imaging sensors have used either analytical solutions to the diffusion equation or simplified monte carlo electron transport models. These methods are computationally attractive and highly useful but may be complemented using more physically detailed models based on TCAD simulations of the devices.

Here we present initial results from a model which employs a full transient numerical solution of the classical semiconductor equations to model charge collection in device pixels under stimulation from initially Gaussian photogenerated charge clouds, using commercial TCAD software. Realistic device geometries and doping are included. By mapping the pixel response to different initial interaction positions and charge cloud sizes, the charge splitting behaviour of the model sensor under various illuminations and operating conditions is investigated.

Experimental validation of the model is presented from an e2v CCD30-11 device under varying substrate bias, illuminated using an Fe-55 source.

Keywords: CCD, X-ray, Charge Collection, Simulation, TCAD, Silvaco

1. INTRODUCTION

Knowledge of the charge collection characteristics of a pixellated detector is of high importance in applications involving single X-ray photon counting. In some cases, a relatively large degree of charge spreading is desirable, when attempting to obtain sub-pixel resolution by a centroiding technique.[1] However, when attempting to obtain the maximum possible energy resolution, it is preferable to have little or no signal splitting between pixels, due to readout noise and dark current implications. The exact charge splitting behaviour of a detector in response to an X-ray stimulus is dependent on the interaction position within the device of the incident photon in relation to the collecting field structure of the device, which in turn depends on the energy of the photon.

Event fitting[2] or spectral redistribution correction[3] algorithms are generally used to correct for charge splitting in spectroscopic applications, but both rely on empirical measurements of the device to obtain the necessary calibration inputs (in the case of event fitting, sets of thresholds to determine event grades are needed, in the case of spectrum correction, knowledge of the response matrix of the device to monoenergetic radiation is required). A predictive tool for charge splitting requiring fewer test measurements would be of value in preselection of device designs for a specific use case.

In this paper we outline the initial work towards realistic device simulations aimed specifically at the investigation of charge collection from X-ray photons. We first briefly review some of the existing work regarding X-rays in CCDs, then describe our own approach. We demonstrate a specific case of experimental validation of the simulation method, before finally evaluating the strengths and weaknesses of the approach and discussing ongoing work.

* daniel.weatherill@open.ac.uk, +44(0)1908 653444

2. REVIEW OF CHARGE COLLECTION SIMULATIONS

Various approaches to simulating the charge collection process in pixellated detectors have been taken by previous authors. McCarthy et al.[4] developed a simulation where a CCD device was divided into a series of layers (substrate, field free region, and depletion region); the spreading of the charge cloud was treated separately in each layer, assuming approximately gaussian spreading in the field free region and exactly gaussian spreading in the depletion region, with radii based on suitable physical considerations. Initial photon positions and charge cloud sizes were selected using monte carlo methods, and from the resulting simulation representative spectra were produced.

A related approach, still based on a "layer" device model, was taken by Pavlov and Nousek.[5] A solution to the diffusion equation in the field free region was obtained using a Fourier series approach, and by convolving the resulting charge distribution with exact gaussian spreading within the depleted layer, a fully analytical (though not closed-form) expression for the expected charge distribution at the collection gates (given an initial photon position and energy) was found. Further integration of this expression allows averages over pixel interaction position to be calculated, which are useful in the determination of event thresholds and response functions.

This work was successfully used in a simulator for the Advanced CCD Imaging Spectrometer (ACIS) aboard the *Chandra* mission. This simulator was used to construct the full response matrix of the ACIS detector from monochromatic calibration data.[6] The disadvantage of all "layer" -type models, is that it is not entirely clear how to properly include the edge effects of the collecting fields. This is of particular interest when considering devices where the collection properties are determined in large part by doping, rather than potentials applied to gates (for example, some CMOS-APS devices and Inverted Mode Operation (IMO) CCDs[7]).

Kreisler et al.[8] performed finite element simulations of the MEDIPIX detector using the adjoint formulation of the drift - diffusion equations,[9] which is computationally advantageous in that a single transient calculation can account in principle for all possible interaction depths (by solving for the adjoint charge density rather than the density). Use of the adjoint method would in principle be a large advantage to the work described here, though in many respects the motivation of Kreisler et al.'s work is similar.

3. SIMULATION METHODOLOGY

All the work described here was carried out using the ATLAS device simulation software from Silvaco. In order to explore the collection of charge from an X-ray photon, a mechanism was needed to inject shaped charge clouds into the device mesh at the beginning of the transient simulation. This is not provided natively by ATLAS, but a facility is included for the user to introduce arbitrary photogeneration by writing a function in the C programming language. There is no way to pass any user defined arguments to this function during the simulation run, so a new function is needed whenever any parameters of the generation (initial position, initial size, initial charge density etc) are changed. In our simulations, a fairly straightforward Python script is used to generate the appropriate C file from a template with the appropriate parameters.

At present, we have implemented uniform ellipsoidal and gaussian initial charge cloud shapes.

Following previous authors,[4] we assign the initial size of the charge cloud r_i based on the incident photon energy E using the semi empirical range formula due to Everhart and Hoff:[10]

$$r_i = k \times \left(\frac{E}{E_0} \right)^{\alpha} \tag{1}$$

with $\alpha = 1.75$, $k = 4.4\,\mathrm{nm}$ and $E_0 = 1.00\,\mathrm{keV}$.

Our device simulations are implemented as two separate 2D structures, which seems justified since the electric fields and doping profiles are all defined along perpendicular lines and appear semi infinite from the perspective of the other direction (especially when we are concerned only with collection of charge and not interested in the storage volume), and it is assumed that the diffusivity and mobility of an epitaxially constructed device will be isotropic, at least in both of the lateral directions. Field dependent mobility is included using the Klasssen model.[11] Full 3D simulation is an area which may be investigated in future work, though it is computationally significantly more expensive.

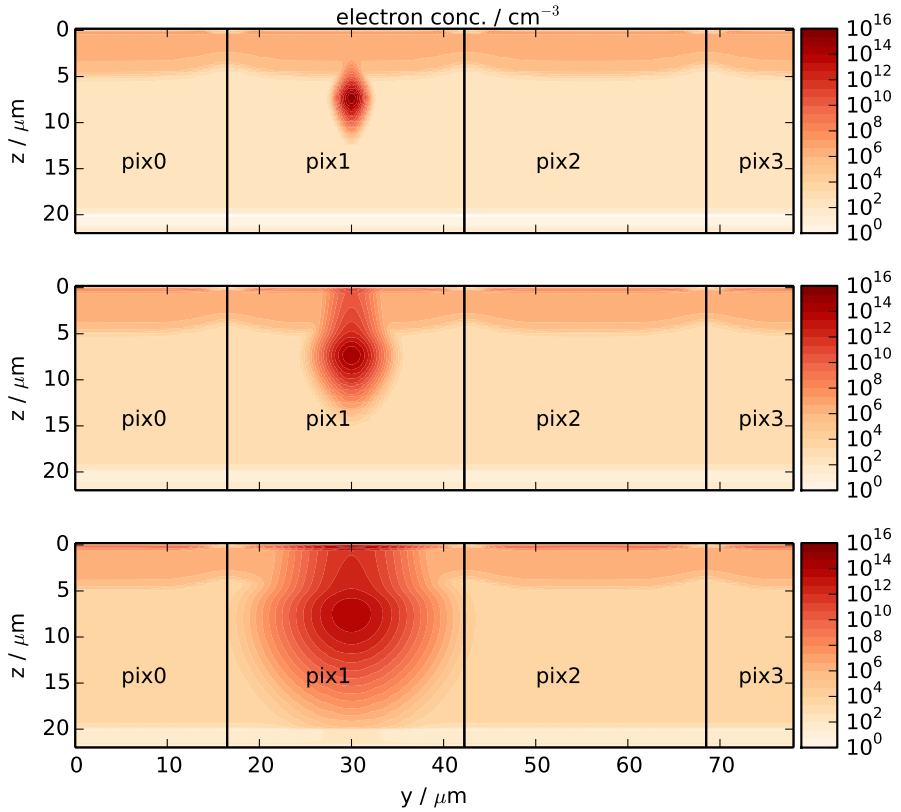

Figure 1: Transient simulation of charge collection, showing the evolution of a charge cloud at sequential time steps during collection. The time steps are approximately 10^{-9} s apart.

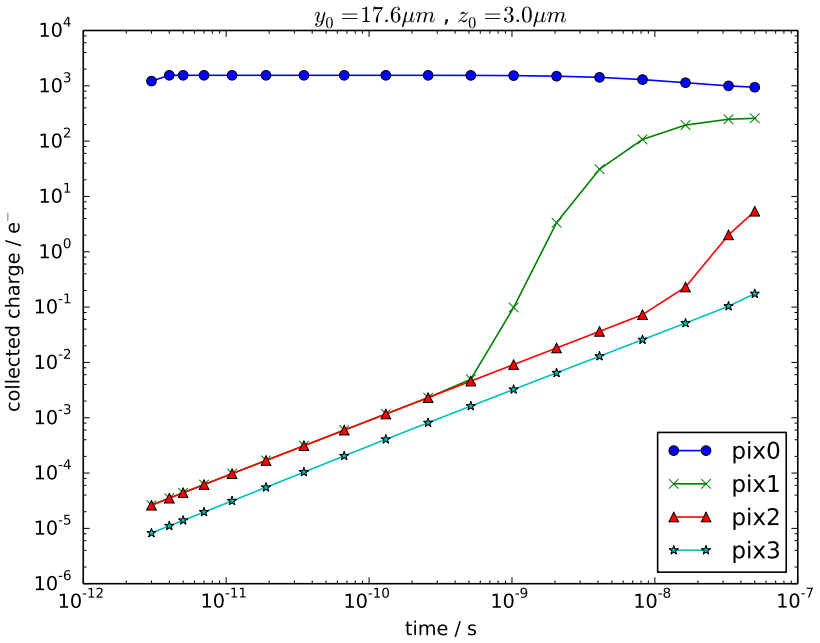

Figure 2: Integrated charge collected in pixels during a transient simulation.

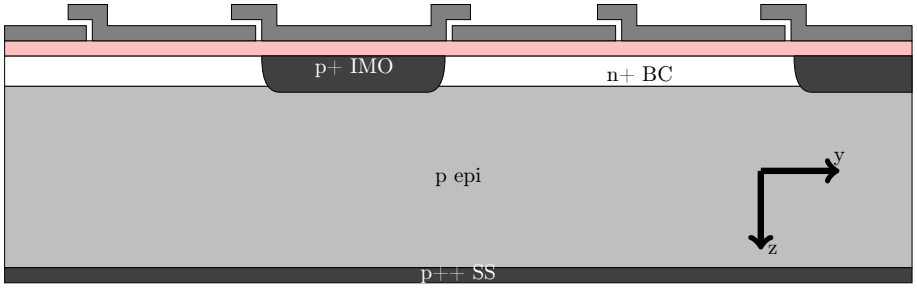

(a) parallel direction (y)

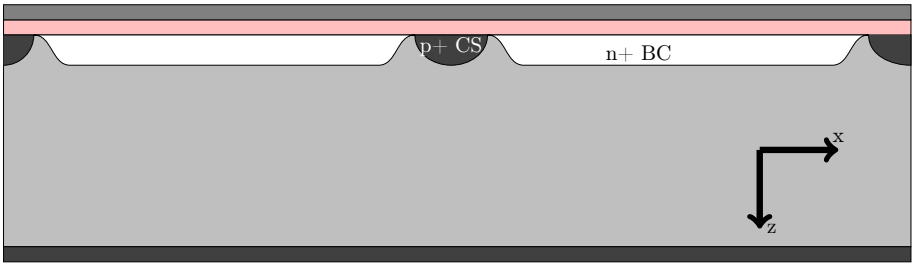

(b) serial direction (x)

Figure 3: Schematic representation of IMO device in parallel and serial transfer directions. IMO - Inverted Mode Operation implant, BC - Buried Channel, SS - substrate, CS - channel stop

After the photogeneration stage, a transient simulation is run, solving the continuity and drift diffusion equations for holes and electrons for a suitably long time (see Figure 1) . The signal in each pixel after collection is measured by numerically integrating the electron density over suitable areas of the mesh (see Figure 2). Our simulations contain 4 pixels in the parallel transfer direction (labelled pix0, pix1, pix2 and pix3 in Figure 2), and three pixels in the serial direction.

Simulations can be run with initial positions selected systematically, to map out the charge spreading properties of the device at a particular energy. Repeating this over many different input energies would in principle allow mapping of the device response function over a range of energies of interest.

Another possibility is to select interaction positions and electron number from appropriately weighted random samples, in order to simulate the same energy spectrum we should obtain from e.g. a calibration source (in this case, Fe-55). We choose initial electron number distribution by applying appropriate Fano variation to the expected energies, obtaining electron number distributions. We then choose interaction depths by selecting from an exponential distribution with the correct absorption length in silicon, and lateral positions are sampled from a random uniform distribution.

4. SIMULATING THE CCD30-11

The CCD30-11 is an Advanced Inverted Mode Operation (AIMO) CCD produced by e2v technologies, UK. A basic sketch of the construction of an IMO device is shown in Figure 3.

Hereafter, the parallel transfer direction is referred to as y, the serial transfer direction as x, and the depth as z. The doping profiles in the model device are reasonably realistic and informed by consultation with e2v engineers, but are composed of gaussian and complementary error function distributions only (i.e. no process simulation was performed). The Inverted Mode Operation and buried channel implants are included in as much detail as practicable (see Figure 4). The device is depleted through manipulation of the electron Quasi-Fermi Level and then biased: in this case with a positive substrate voltage, and all the collecting gates held at ground (a typical condition when using the device in IMO). An example of the resulting potential distribution is shown in Figure 5.

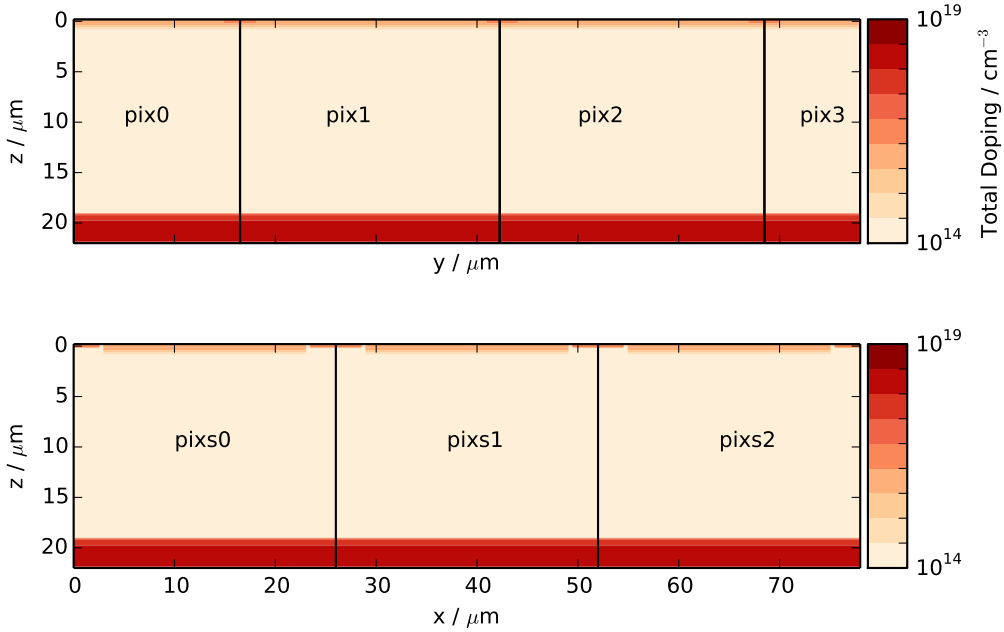

Figure 4: Doping profiles in the modelled CCD30-11 device

V_{ss}=9.39V

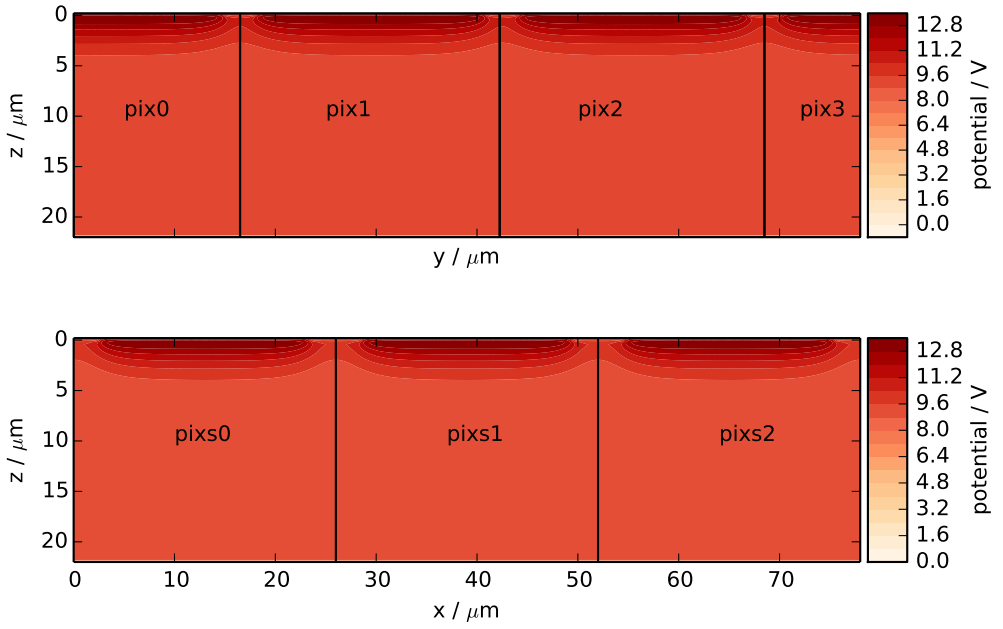

Figure 5: Potential distribution in the depleted device

5. EXPERIMENTAL RESULTS

An e2v CCD30-11 was illuminated with an Fe-55 source, with part of the device being covered by a plastic mask to allow image sections to be used for dark current and offset correction. The device was cooled thermo-electrically to $-40\,^{\circ}\mathrm{C}$. 2000 images were taken at 12 different substrate voltages between 7 V and 10.5 V with respect to the image clock voltages. This resulted in a corpus of $\sim 10^6$ identifiable X-ray interactions for each voltage in the resulting images. There is a particular error associated with events which arrive whilst the device is being read out, which are spurious to the analysis. A sufficiently long integration time (60 s, compared with a readout time of 0.56 s) reduces this error to below the 1% level. It is hoped that with future work, a method can be developed to distinguish these events in post processing, since they are in principle amenable to investigation through the same methodology described here.

After subtraction of offset and dark current, X-ray events within images were located by first taking a threshold 4σ above the dark current, where σ is the standard deviation of a gaussian fit to the dark current peak. A Laplace filter and local maximum filter were then used to identify events. The locating algorithm was checked visually on 40 images for accuracy.

In order to characterise the degree of charge spreading in the data, we analyse the detected events using image moments. Although this technique is likely not as sensitive as e.g. fitting the parameters of a known function to the event shape, it has the advantage that we have not had to assume any particular shape for the events (e.g. Gaussian).

The raw image moments M_{ij} of a 2D image $I(x, y)$ are defined by:[12]

$$M_{ij} = \sum_x \sum_y x^i \cdot y^j \cdot I(x, y) \tag{2}$$

Following on from this definition, we define the *central moments* μ_{ij} by:

$$\mu_{ij} = \sum_x \sum_y (x - \bar{x})^i \cdot (y - \bar{y})^j \cdot I(x, y) \tag{3}$$

where the *centroids* $(\bar{x}, \bar{y})$ are given by:

$$\bar{x} = \frac{M_{10}}{M_{00}}\,;\, \bar{y} = \frac{M_{01}}{M_{00}} \tag{4}$$

In our case, each image is an X-ray photon event. We are especially interested in the moments μ_{20} and μ_{02} because they are the closest to a measure of variance, or "spread".

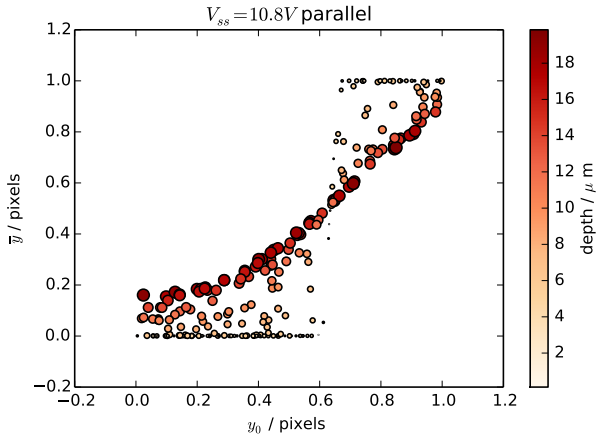

Figure 6: True position (y_0) vs calculated centroid ($\bar{y}$) for simulated photons, showing interaction depth as size and colour of data points.

6. ANALYSIS

It can be shown[12] that:

$$\mu_{20} = M_{20} - \bar{x} \cdot M_{10} \equiv M_{20} - \bar{x}^2 M_{00} \tag{5}$$

and similarly for μ_{02}. As illustrated by Figure 6, the extent to which the linearly calculated centroid position $\bar{y}$ represents the true interaction position y_0 depends on the depth of the particular interaction z, which is unknown on an event by event basis experimentally. It is therefore inappropriate to simply analyse distributions of μ_{20} in isolation, since they implicitly depend upon this relationship. Instead, we should assess the spreading based on a quantity which retains the desirable translation invariance of μ_{20}, but which also accounts for the fact that we cannot rely on our measurements of $\bar{y}$ being true estimates of y_0.

Consider an image reduced along one axis then normalised (i.e. $M_{00} = \sum_x I(x) = 1$), then we can rewrite (5) as:

$$\mu_{20} = \sum_x I(x) \cdot x^2 - \bar{x}^2 \tag{6}$$

If we further suppose that

$$\sum_x I(x) \cdot x^2 = \sum_x I(x) \cdot x = \bar{x} \tag{7}$$

then we obtain

$$\mu_{20} = \bar{x}(1 - \bar{x}) \equiv \frac{1}{4} - \left(\bar{x} - \frac{1}{2}\right)^2 \tag{8}$$

The condition (7) may be satisfied by several situations: the image $I(x)$ is identically zero; the image is a delta-like function at the origin (i.e. an isolated x-ray event), or the image is an event equally split between pixels. We will refer to this as the "zero spread condition" (ZSC). The level of deviation from this condition is an indication of both the quantity of spreading and the quality of the linear centroid $\bar{x}$ as an estimate for the true interaction location x_0. By fitting a parabola

$$\nu(\bar{x}) = a_0 \bar{x}^2 + a_1 \bar{x} + a_2 \equiv -\frac{a_1^2}{4a_0} + \frac{a_2}{a_0} + a_0 \left(\bar{x} + \frac{a_1}{2a_0}\right)^2 \tag{9}$$

to the graph of μ_{20} against $\bar{x}$ (see Figure 7), we can obtain a "spreading measure", ω, based on the difference between the fitted coefficients and the ZSC:

$$\omega = \frac{1}{4} + \frac{a_1^2}{4a_0} + \frac{a_2}{a_0} \tag{10}$$

This measure fits the desired criteria of not assuming implicitly $\bar{y} = y_0$. The size of ω calculated for various substrate voltages agrees reasonably well between simulation and experiment (see Figure 8), though unfortunately there is not a substantial variation in the measure over a range of substrate voltages specified for normal operation. This is to be expected for the IMO device where the substrate bias is above the inversion threshold and the collecting fields are almost exclusively defined by the implants. Notably the position and magnitude of the peak in Figure 8 are quite well predicted by simulation, and show that as the substrate bias passes into inversion, significant excess spreading of events is taking place. This gives good support to the validity of the simulation techniques to be used on other devices and operating conditions in future work.

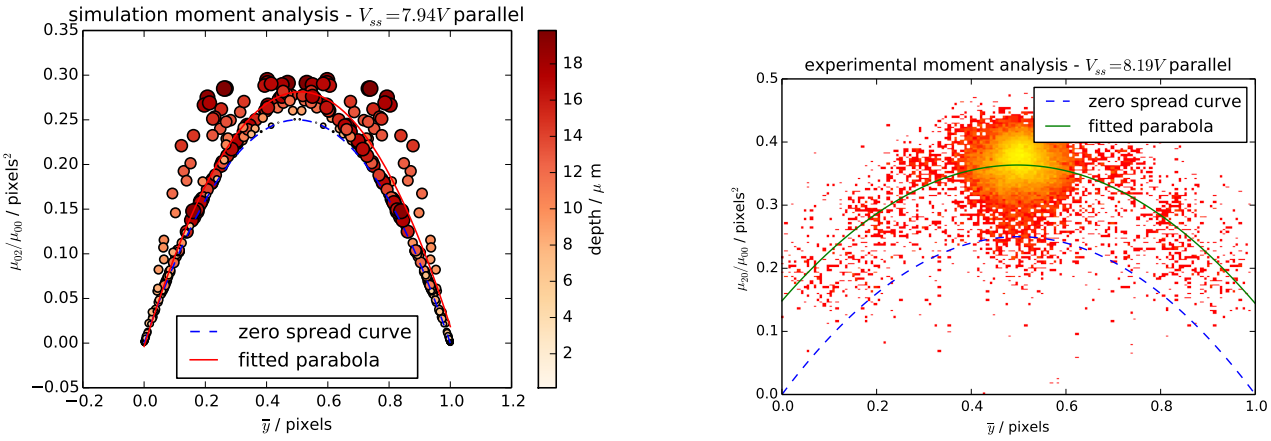

(a) Simulated photons

(b) Experiment. Colour shows number of events

Figure 7: Example calculated centroid vs normalised second central moment ($\frac{\mu_{02}}{\mu_{00}}$) plots.

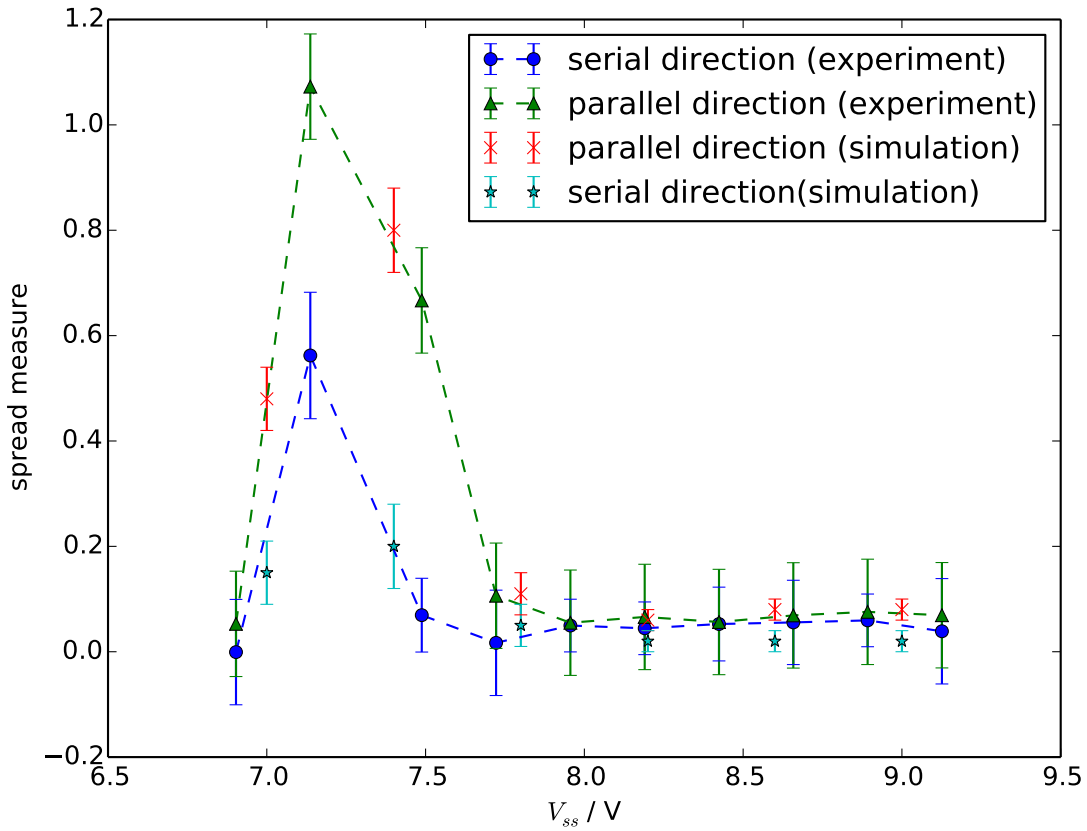

Figure 8: Substrate voltage vs. spread measure, comparing simulation and experimental results. Error bars are calculated from the covariance of the least squares fit.

7. CONCLUSIONS

We have demonstrated (to proof of concept) level the modelling of charge collection from X-ray photons in a CCD using a TCAD model of the sensor, and shown that for a particular measure of charge spreading, experimental results are well matched in a particular device. Though the sensor used in this experimental work is not the most advantageous to demonstrate the change in charge spreading with substrate potential (being an Inverted Mode Operation device), it is nonetheless difficult to simulate using previous techniques. We believe our simulation method to be useful enough to apply to other devices, including deep depletion back illuminated EM-CCD devices and CMOS Active Pixel Sensor devices.

We hope to both apply this simulation technique to more devices and improve the utility of the parameters which we can extract from it. We hope to include accurate predictions of X-ray Point Spread Function (PSF), Quantum Efficiency (QE), and perhaps eventually portions of the full monoenergetic device response functions.

Improvements to the method are also underway, including investigating the potential of leveraging the adjoint formulation to improve the completeness of the modelling data.

8. ACKNOWLEDGEMENTS

The authors would like to thank Mr David Burt of e2v technologies for technical input and advice about the CCD30-11, Dr Douglas Jordan and Dr James Endicott of e2v technologies and Dr Ivan Kotov of Brookhaven National Laboratory for valuable discussions. We would also like to acknowledge the funding from the Science and Technology Facilities Council (STFC) for this work.

REFERENCES

[1] M. Soman, D. Hall, J. Tutt, N. Murray, A. Holland, T. Schmitt, J. Raabe, and B. Schmitt, "Developing a ccd camera with high spatial resolution for rixs in the soft x-ray range," *Nuclear Instruments and Methods in Physics Research Section A: Accelerators, Spectrometers, Detectors and Associated Equipment*, vol. 731, no. 0, pp. 47 – 52, 2013. PIXEL 2012.

[2] A. Owens, T. Mineo, K. J. McCarthy, and A. Wells, "Event recognition in x-ray ccds," *Nuclear Instruments and Methods in Physics Research Section A: Accelerators, Spectrometers, Detectors and Associated Equipment*, vol. 346, no. 1–2, pp. 353 – 365, 1994.

[3] P. Sievers, T. Weber, T. Michel, J. Klammer, L. Büermann, and G. Anton, "Bayesian deconvolution as a method for the spectroscopy of x-rays with highly pixelated photon counting detectors," *Journal of Instrumentation*, vol. 7, no. 03, p. P03003, 2012.

[4] K. J. McCarthy, A. Owens, A. Holland, and A. A. Wells, "Modelling the x-ray response of charge coupled devices," *Nuclear Instruments and Methods in Physics Research Section A: Accelerators, Spectrometers, Detectors and Associated Equipment*, vol. 362, no. 2–3, pp. 538 – 546, 1995.

[5] G. G. Pavlov and J. A. Nousek, "Charge diffusion in ccd x-ray detectors," *Nuclear Instruments and Methods in Physics Research Section A: Accelerators, Spectrometers, Detectors and Associated Equipment*, vol. 428, no. 2–3, pp. 348–366, 1999.

[6] L. K. Townsley, P. S. Broos, G. Chartas, E. Moskalenko, J. A. Nousek, and G. G. Pavlov, "Simulating CCDs for the Chandra Advanced CCD Imaging Spectrometer," *Nuclear Instruments and Methods in Physics Research A*, vol. 486, pp. 716–750, July 2002.

[7] J. Janesick, T. Elliott, G. Frasehetti, S. Collins, M. Blouke, and B. Corrie, "Charge-coupled device pinning technologies," 1989.

[8] B. Kreisler, J. Durst, T. Michel, and G. Anton, "Generalised adjoint simulation of induced signals in semiconductor x-ray pixel detectors," *Journal of Instrumentation*, vol. 3, no. 11, p. P11002, 2008.

[9] T. Prettyman, "Method for mapping charge pulses in semiconductor radiation detectors," *Nuclear Instruments and Methods in Physics Research Section A: Accelerators, Spectrometers, Detectors and Associated Equipment*, vol. 422, no. 1–3, pp. 232–237, 1999.

[10] T. E. Everhart and P. H. Hoff, "Determination of kilovolt electron energy dissipation vs penetration distance in solid materials," *Journal of Applied Physics*, vol. 42, no. 13, pp. 5837–5846, 1971.

[11] D. Klaassen, "A unified mobility model for device simulation—i. model equations and concentration dependence," *Solid-State Electronics*, vol. 35, no. 7, pp. 953 – 959, 1992.

[12] R. Mukundan and K. Ramakrishnan, *Moment functions in image analysis: theory and applications*, vol. 100. World Scientific, 1998.